Decision-Directed Burst-Mode Carrier Synchronization Techniques

Michael P. Fitz, *Member, IEEE,* and William C. Lindsey, *Fellow, IEEE*

Abstract— **In burst-mode communication systems rapid carrier and clock synchronization is essential. In many practical applications an accurate phase reference can rapidly be obtained resulting in up to a 2–3 dB performance improvement over differentially coherent detection. This paper presents a decision-directed, digitally implemented carrier synchronizer for channels with both frequency and phase uncertainty. This combined algorithm and its derivatives are analyzed with respect to the achievable carrier acquisition time and the resulting bit error probability. For certain data rates (approximately 50 MSps or less) this algorithm can be implemented using CMOS gate array technology. As examples BPSK and QPSK modulation formats are studied herein and compared to their differentially coherent counterparts of DPSK and DQPSK.**

I. Introduction

MODEMS for burst-mode communications such as time-division multiple-access (TDMA) or slow frequency hopping (FH) are used for many applications. The best performance is realized with phase-coherent demodulation [1]; however, the traditional methods of carrier and clock synchronization using phase-locked loops cannot provide rapid acquisition with high probability when operating in the burst mode. The phase-locked loop (PLL) exhibits the hang-up phenomena [4], [5]. Hang-up is the prolonged dwell at large phase errors by the PLL. To avoid this phenomenon most burst-mode modem designs have not incorporated PLL's for carrier synchronization.

Certain techniques have been investigated to circumvent the problems caused by this hang-up phenomena. The initial research in this area focused on quantifying the hang-up phenomena [5] and deriving ad hoc structures which mitigated the effects of hang-up. Unaided acquisition requires the transmission of a long preamble if a high probability of attaining phase lock is required. This characteristic either reduces the throughput data rate or increases the burst length. Depending on the application, either one or both of these alternatives reduces the attractiveness of using a PLL for carrier synchronization in burst-mode communications. The ad hoc structures provide the desired performance improvement but do it with a significant increase in complexity and cost. Tuned tank circuits which ring at the proper frequency [10] have also been considered. The tuned tank synchronization architecture performance and complexity is highly dependent on the implementation.

A third method utilized in burst-mode modems is differentially coherent detection of PSK modulation [1]. This implementation has several advantages. First, the receiver is very simple. Second, since the previous symbol phase is the reference for detection of the current symbol, only one symbol of preamble is required for carrier synchronization. This modulation format is frequently used in slow FH modems where the clock epoch is known *a priori*. In a slow FH system, several to hundreds of symbols are transmitted each hop but the hop rate is fast enough to maintain the desired repeat-back jamming performance. This hop rate in conjunction with the hang-up phenomena precludes a PLL based modem. The performance difference between differential coherent detection and coherent detection is 2–3 dB in coded (high symbol error rate) systems. This 2–3 dB performance gain is the motivation for this work

A current trend in carrier synchronization research is the investigation of algorithms based on the maximum likelihood (ML) estimate of the carrier phase [7]–[9], [11], [13]. These algorithms typically operate on both the amplitude and phase of the received signal and do not contain feedback in the sense of the PLL. Actually, the most conspicuous characteristic of these estimation structures is the absence of a locally generated sinusoid (no numerically or voltage-controlled oscillator is required). The nonlinear phase estimator [11] is the large noise approximation to the ML estimator, while the decision-directed estimator [9] is the small noise approximation. In [11], the nonlinear estimator has been thoroughly characterized but similar work has not been done for the decision-directed estimator.

The decision-directed phase estimator is of practical interest due to its applicability to all modulation types and its superior performance at high E_b/N_0. Decision-directed phase estimation is a very simple method of carrier synchronization. It can be applied in modems of all modulation types from BPSK to combined amplitude and phase modulation. Since the decision-directed estimator is the small noise approximation to the ML phase estimator, it has near optimum performance at high E_b/N_0. This is particularly true for higher order (MPSK) and non-phase shift modulations, since the noise enhancement in nonlinear carrier synchronizers significantly degrades the performance. Decision-directed phase estimation

Paper approved by the Editor for Synchronization Systems and Techniques of the IEEE Communications Society. Manuscript received October 5, 1989; revised October 29, 1990 and April 16, 1991. This work was supported in part by a TRW Doctoral Fellowship and the National Science Foundation under Grant NCR-9010239.

M. P. Fitz is with the School of Electrical Engineering, Purdue University, West Lafayette, IN 47907.

W. C. Lindsey is with the University of Southern California, Los Angeles, CA 90089. He is also with LinCom Corporation, Los Angeles, CA 90056.

IEEE Log Number 9201643.

has a limitation of supporting only causal estimation structures (that is an inherent advantage of [11]). Decision-directed processing is advantageous in many situations but causal operation is required.

A desirable feature for modern modems is the extensive use of digital processing in their implementation. Gate array technology is mature and the use of these technologies in modems can reduce the size and weight as well as providing more reliable operation. The ML-based architectures are ideally suited for digital implementation because of the minimal signal feedback [13], [6] and the ability of ROM's to provide a wide range of transfer functions [11]. Because of this fact the physical implementation of modems can be significantly simplified.

The work herein essentially extends the theory of digitally implemented phase estimators in two ways. The first is the presentation of a phase and frequency estimation algorithm which can acquire and track a signal with a frequency offset. The previous work either assumes that the frequency uncertainty was small [9], [13], hence neglected, or that the estimator structure was noncasual [11]. The algorithm presented in this paper is both causal and has a performance which is independent[1] of the frequency offset. The second new result is the derivation of the acquisition performance of these estimators and the resultant data-aided[2] BEP learning curves. The acquisition performance characterization considerably extends the work in [9], [11], [12], [17]. The results presented in this paper are for BPSK and QPSK modulations, although a majority of the results can be generalized to any linearly modulated signal set [6].

The paper is organized as follows. Section II describes the signal, channel and receiver models which provide the basis for the ensuing analysis. Section III presents the new frequency tracking phase estimator (the combined algorithm) and reviews a special case of this combined algorithm (the exponentially weighted algorithm [9]). The resultant RMS phase error performance of the combined algorithm for an unmodulated carrier input is also analyzed. Section IV derives the data-aided BEP learning curves and presents simulation results for the overall BEP for BPSK and QPSK modulations when the algorithms in Section III are utilized for phase synchronization. Section V presents the conclusions of this work.

II. Analysis Models

This paper focuses on digital receiver implementations. For the wideband AWGN channel this receiver can be modeled by Fig. 1. The modulation signal $z(t)$ represents the transmitted BPSK or QPSK waveforms in complex baseband form. In Fig. 1, the complex exponential multiplying $z(t)$ models the unknown phase and frequency induced by the channel. The noise is modeled as additive white Gaussian (AWG) and the receiver filter is matched to the modulation pulse shape. The A/D converter samples the matched filter output and this sampled signal is used both to estimate the phase and demodulate the data sequence.

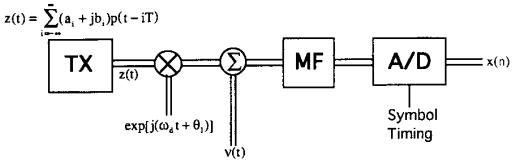

Fig. 1. Analysis model for an AWGN channel.

The major assumption made for the results derived in this paper is that the symbol timing (clock synchronization) is known. In general this is not the case; however, in certain burst-mode communication systems applications it is the case. TDMA systems typically employ highly stable timing sources [11] and the timing is derived during the preliminary bursts and periodically updated. The same is true of a slow FHSS system. For FH systems employed for antijam (AJ) purposes the timing estimation must be robust and hence it is not desirable to estimate the timing each hop. These systems will also estimate the symbol timing prior to data transmission and periodically update the estimate. The results of this paper can easily be generalized to other communication systems if symbol timing acquisition is accomplished prior to the phase acquisition. Hence, assuming a known symbol timing does not reduce the significance of this research. The known timing assumption implies that one sample per symbol provides sufficient statistics for both symbol and carrier phase estimation. This will become more evident later on in this section.

If symbol timing is known and the pulse shape satisfies the Nyquist criterion for zero ISI, then the matched filter output samples have a succinct form. The general form is

$$x(n) = (a_n + jb_n)\sqrt{E_b}\rho(\omega_o)\exp[j(\omega_o n + \theta_o)] + \nu(n) \quad (1)$$

where E_b is the bit energy, n is the sample number, a_n and b_n are i.i.d. binary modulation sequences ($b_n = 0$ for BPSK), $\omega_o = \omega_d T$ is the phase rotation per symbol, $\rho(\omega_o)$ is the mismatch loss of the matched filter due to frequency offset, and θ_0 is the carrier phase at $n = 0$. It is easy to show that $\nu(n)$ is a zero mean, delta correlated, discrete time, Gaussian random process with variance N_0. In the slow FHSS system, ideal rectangular pulses are a good model. Considering this example, the matched filter output samples, given in (1), have the form

$$\begin{aligned} x(n) &= (a_n + jb_n)\cdot\sqrt{E_b}\cdot\operatorname{sinc}\left(\frac{\omega_o}{2}\right) \\ &\quad\cdot\exp\left\{j\left(\omega_o n + \frac{\omega_o}{2} + \theta_1\right)\right\} + \nu(n) \\ &= (a_n + jb_n)\cdot\sqrt{E_b}\cdot\operatorname{sinc}\left(\frac{\omega_o}{2}\right)k^n\exp\{j\theta_0\} + \nu(n) \end{aligned}$$

where $k = \exp[j\omega_o]$. The frequency offset (ω_o) can be induced by Doppler shift due to relative motion between transmitter and receiver or manufacturing tolerance of the frequency sources. The phase process in this model is a constant.

Equation (1) demonstrates that the matched filter output sample has the form of a complex sinusoidal sequence in

[1] The algorithm is independent of frequency offset if subsymbol processing is used when large frequency errors are possible. See Section II.

[2] By data-aided we mean that the modulation preamble is known *a priori* at the receiver or perfectly estimated when utilizing decision-directed feedback.

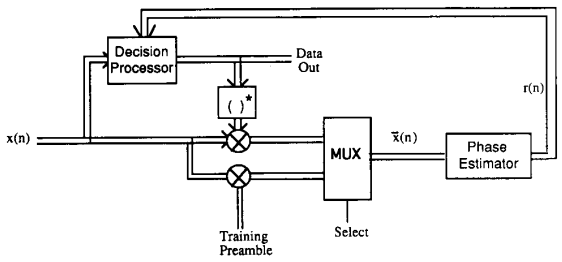

Fig. 2. The proposed demodulator block diagram.

AWGN with a random modulation symbol on each sample. If the modulation is known (a training preamble) or if the modulation can be removed, the resultant signal will be a complex sinusoid in additive noise. The phase of this signal can be estimated by the PLL or planar filtering. The two most prevalent methods of removing the modulation are nonlinear processing [11] or decision-directed processing [9]. This paper will concentrate on phase estimation techniques applicable to a decision-directed architecture. The block diagram of the demodulator architecture being proposed is seen in Fig. 2. Ideally, $\overline{x}(n)$ will be a discrete time complex sinusoid in noise having the form

$$\overline{x}(n) = \sqrt{E_s}\rho(\omega_0)k^n \exp[j\theta_0] + \nu(n)$$

where E_s is the symbol energy.[3] The phase estimator processes both the I and Q components (a planar filter) so when the modulation is perfectly removed the smoothed phase reference will have the form

$$r(n) = \sqrt{G(n)E_s}\rho(\omega_0)k^n \exp[j(\theta_0 + \theta_e(n))] + \nu_r(n)$$

where $\theta_e(n)$ is the phase estimate bias. For analytic simplicity $r(n)$ is appropriately scaled so $\nu_r(n)$ has a variance of N_0. Because of this scaling, the function $G(n)$ is the signal-to-noise ratio (SNR) gain of the phase estimator. $G(n)$ is a measure of the improvement in the reference SNR compared to the matched filter output SNR. The analogous quantity to $G(n)$ in the PLL is the ratio of the symbol rate to the loop bandwidth. $G(n)$ is used in Section IV to find an approximate BEP expression.

III. Digital Carrier Synchronization

A. Phase and Frequency Estimation

The burst synchronization problem addressed in this paper corresponds to the design of a frequency tracking, rapidly acquiring, causal (due to the decision-directed processing), digital carrier synchronizer. The synchronizer is analogous to a Type II PLL since the estimate remains unbiased in the presence of a frequency offset. Much of the previous work is not applicable to this problem. References [7], [9], [12] considered models with negligible frequency offset and are not applicable. Reference [11] uses nonlinear processing and a symmetric smoothing filter to produce an unbiased phase estimate. But the nonlinear phase estimator [11] has degraded performance if the frequency offset is a large portion of the smoothing filter bandwidth. This degradation is approximately proportional to

$$\rho(\omega_o) = \operatorname{sinc}^2\left(\frac{\omega_o MN}{2}\right)$$

where M is the alphabet size and N is the number of taps in the smoothing filter. Hence, accurate phase estimation with significant frequency offset is not possible using the nonlinear estimation method suggested in [11]. The research presented in this paper is motivated by the search (need) for a frequency tracking phase estimator.

Significant insight into carrier synchronization can be derived from optimal filter theory. When using an error-free, decision-directed algorithm, carrier synchronization can be cast as a problem in prediction filtering. This idea is developed in [13] and a generalized Kalman filter for carrier synchronization results. Unfortunately the Kalman filter has two shortcomings for burst mode synchronization: 1) for estimation with a frequency offset an additional state variable must be added to the Kalman model to represent k [13] and 2) the Kalman filter is a recursive estimator with acquisition characteristics highly dependent on the initial estimate. The sampled signal and noise models presented in Section II are cyclo-stationary random processes and linearly dependent on both k and $\exp[j\theta_0]$. These characteristics imply that minimum mean square error (MMSE) linear prediction [3], [21] can provide some insight into practical digital phase estimators.

Examination of the MMSE prediction filter provides significant insight into the estimation of k and θ_0. For the signal model presented in Section II with the modulation perfectly known and assuming N symbols have been received, the corresponding prediction filter normal equations for the estimator of the $N+1$ received symbol are of the form [3]

$$\sum_{i=0}^{N-1} W_i \phi_{\overline{x}}(m-i) = \phi_{\overline{x}}(m+i) \quad \mathbf{0} \le m \le N-1$$

where $\phi_{\overline{x}}(m)$ is the discrete time correlation function of $\overline{x}(n)$. Since

$$\phi_{\overline{x}}(m) = E_s \exp[-j\omega_o m] + N_0\delta(m)$$

the MMSE prediction filter is given by

$$r(N+1) = \frac{1}{NE_s + N_0} \sum_{i=0}^{N-1} k^{i+1}\overline{x}(N-1). \qquad (2)$$

Two important characteristics of this filter structure are each tap weight has a constant magnitude and is a function of k. Even though k and E_s/N_0 are unknown, the characteristics of this MMSE solution can equivalently be utilized to develop rapidly acquiring carrier synchronizers.

Equation (2) can be manipulated to get a practical phase estimation structure. Realizing that carrier synchronization for PSK modulations is only interested in the argument of $r(N+1)$, the constant term in front of the summation is

[3] $E_s = E_b$ for BPSK and $E_s = 2E_b$ for QPSK.

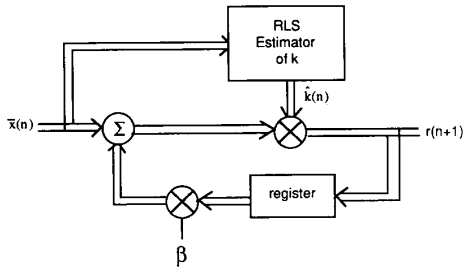

Fig. 3. Combined algorithm block diagram.

irrelevant. This implies that (2) can equivalently be rewritten as

$$\begin{aligned} r(N+1) &= k\sum_{i=0}^{N-1} k^i \bar{x}(N-i) \\ &= k\bar{x}(N) + k\left[k\sum_{i=0}^{N-2} k^i \bar{x}(N-1-i)\right] \\ &= k\bar{x}(N) + kr(N). \end{aligned}$$

This equation illustrates an important point that if k is known, then the linear MMSE estimator is expressed in a simple recursive form. In practice k is not known, but using a recursive estimator of k and a fading factor results in a practical carrier synchronization having the form

$$\begin{aligned} &\hat{\theta}(n) \triangleq \arg[r(n)] \\ &r(n) = \hat{k}(n)[\beta r(n-1) + \bar{x}(n-1)] \end{aligned} \tag{3}$$

where $\hat{\theta}$ is the phase estimate at time n, $\hat{k}(n)$ is the estimate of k at time n, and β is the phase estimate fading factor ($\mathbf{0} \leq \beta < 1$). Due to the recursive nature of this algorithm, if k is perfectly estimated the coefficients on each matched filter output, $x(n-i)$, will be k^i as in (2). The fading factor β controls the memory length of the filter. The choice of β is a compromise between averaging over many symbols ($\beta \to 1$) and reducing the cumulative effect of the noise associated with $\hat{k}(n)(\beta \to \mathbf{0})$. The algorithm of (3) will be referred to as the combined algorithm since it combines the exponentially weighted (EW) estimator [9] with an estimate of k. Fig. 3 demonstrates the inherent simplicity of this digital carrier synchronizer.

The remaining portion of this section will discuss the various attributes of this estimation scheme. First an estimate of k will be developed and analyzed. Then the combined algorithm performance will be assessed and important characteristics highlighted.

B. Estimation of k

An estimate of k must acquire rapidly and be simple to implement for utility in this application. Again, assuming the modulation is perfectly known the calculation of $\hat{k}(n)$ can be formulated in terms of an adaptive linear prediction problem, i.e.,

$$\hat{x}(n+1) = W\bar{x}(n).$$

This is the form of a one step, one tap prediction filter and the MMSE solution is easily shown to be (see (2) with $N = 1$)

$$W_{\text{opt}} \propto k = \exp[j\omega_o].$$

Since rapid acquisition is paramount, the least square (LS) adaptive filters, which exhibit the most rapid convergence to the MMSE solution [2], [3], are most applicable. Considering algorithms which minimize the weighted[4] sum of the square error, i.e.,

$$\epsilon(n) = \sum_{i=1}^{n} \gamma^{n-i} |\bar{x}(i) - \hat{x}(i)|^2$$

$\hat{k}(n)$ has the form [2], [3]

$$\hat{k}(n) = \frac{\sum_{i=1}^{n} \gamma^{n-i} \bar{x}(i)\bar{x}^*(i-1)}{\sum_{i=0}^{n} \gamma^{n-i} |\bar{x}(i)|^2}.$$

Since the denominator is just a term proportional to the power in the sequence $x(n)$ and only the phase of the reference effects the BEP performance, an equivalent estimator is of the form

$$\hat{k}(n) = \frac{\sum_{i=1}^{n} \gamma^{n-i} \bar{x}(i)\bar{x}^*(i-1)}{\left|\sum_{i=1}^{n} \gamma^{n-i} \bar{x}(i)\bar{x}^*(i-1)\right|}.$$

This implies that the normalized frequency estimate has the form

$$\hat{\omega}_0(n) = \arg[\hat{k}(n)] = \arg\left[\sum_{i=1}^{n} \gamma^{n-i} \bar{x}(i)\bar{x}^*(i-1)\right]. \tag{4}$$

This frequency estimation component of the combined algorithm was first presented in [25] and also in [20], but the relationship to the RLS derivation was not recognized.

A closed-form solution for the probability density function (pdf) of $\hat{\omega}_0$ for an estimator performance evaluation was not apparent to the authors. Reference [20] made a Gaussian approximation and calculated the resulting steady-state pdf. Typically, adaptive filter performance and its learning curves are evaluated by Monte Carlo simulation. The estimation error learning curves for this estimator are seen in Figs. 4–5 for various SNR's and $\omega_o = 0.5$ and $\omega_o = 1.0$ radians/sample, respectively. Examination of Figs. 4–5 demonstrates that the rms error produced by (4) is independent of ω_o. These figures demonstrate that this estimator rapidly converges to values very near the optimum Wiener solution ($k = \exp[j\omega_o]$).

[4]The weighting parameter γ permits the estimate to track the instability in the carrier frequency. The parameter γ will only have a significant impact on performance when the burst length is long, or burst to burst tracking is utilized. For this work $\gamma = 1$.

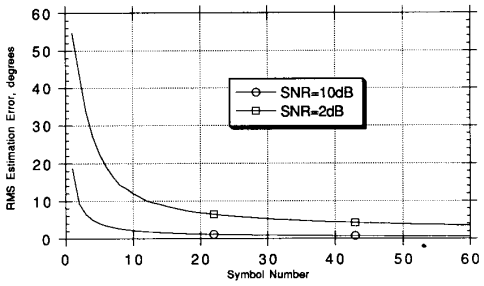

Fig. 4. Learning curves for $\hat{k}$. $\omega_0 = 0.5$ radians/symbol, $\gamma = 1$, 10 000 trials.

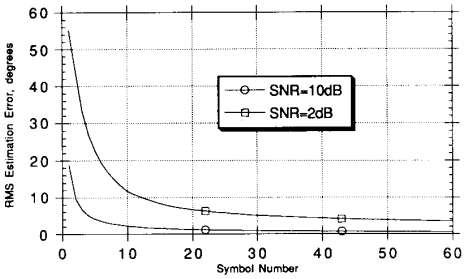

Fig. 5. Learning curves for $\hat{k}$. $\omega_0 = 1.0$ radian/symbol, $\gamma = 1$, 10 000 trials.

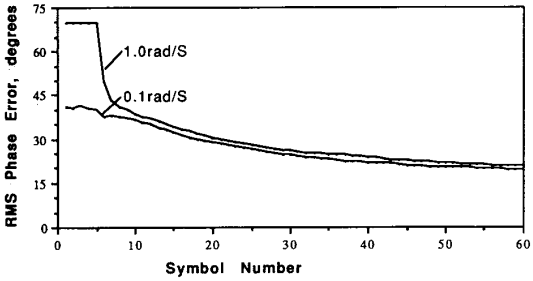

Fig. 6. Combined algorithm learning curves for various frequency offsets. $E_s/N_0 = 2$ dB, $\beta = 0.75$, $kk = 4$, 10 000 trials.

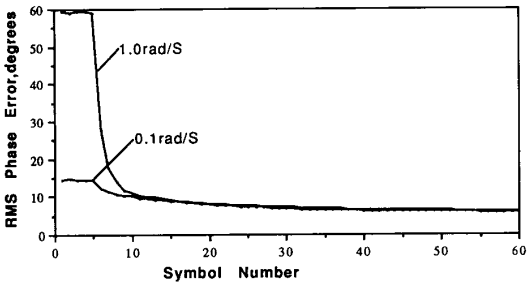

Fig. 7. Combined algorithm learning curves for various frequency offsets. $E_s/N_0 = 10$ dB, $\beta = 0.75$, $kk = 4$, 10 000 trials.

C. Phase and Frequency Estimation

The combined algorithm phase estimator uses the estimate of k given in (4) in the recursive estimator of (3). The initialization of the combined algorithm and the value of β have the greatest impact on the performance of this algorithm. Since the combined algorithm is a recursive estimation algorithm, a poor initial estimate can slow the convergence/acquisition process. Through Monte Carlo computer experiments [6], the combined algorithm was shown to acquire more rapidly if the initial symbols were utilized to produce an estimate of k alone. This algorithm improves the convergence characteristics of the combined algorithm by delaying the application of the exponential weighting until $\hat{k}(n)$ becomes less noisy. In [6] a four-symbol frequency estimation preamble demonstrated the desired performance. The nonlinear nature of this algorithm precludes a numerical analysis but the phase estimation learning curves derived from Monte Carlo simulations are presented in Figs. 6–7. In these figures kk refers to the length of the frequency acquisition preamble and ω_o the phase change per symbol (normalized frequency offset).

The choice of the parameter β determines the performance of the combined phase estimator. At first glance it appears that β determines the bandwidth of the estimator as in [9], but the operation is more subtle. In effect β determines the memory of the estimator. Solving the corresponding difference equation, $r(n+1)$ can be expressed as

$$r(n+1) = \sum_{i=0}^{n} \beta^i \left[\prod_{j=0}^{i} \hat{k}(j) \right] \overline{x}(n-i).$$

In this equation the explicit effect of β can be seen. If β is near unity many samples in the past will contribute to $r(n+1)$ and hence better smoothing of the reference is obtained. Unfortunately since $\hat{k}(j)$ is noisy the values of $\overline{x}(n-i)$ in the past will also be weighted by powers of this noisy estimate. Because of this weighting, contributions from far in the past will be very noisy. Conversely if β is near zero the error due to noise in $\hat{k}(j)$ will be minimized, but less smoothing of $\overline{x}(n)$ occurs. This implies an optimum β exists which minimizes the mean square phase error. Work presented in [6] determined that this optimum value of β is approximately 0.75 for $E_s/N_0 = 2$ dB.

D. Algorithm Characteristics

If k is accurately estimated prior to a burst (or if $\hat{k} = 1$), the algorithm's performance will be very near that of the EW phase estimator [9]. This can be useful in a system application where the frequency sources are stable. Since the expression for $\hat{k}(n)$ determined by (4) is recursive, saving the value of

$$\sum_{i=1}^{n} \gamma^{n-i} \overline{x}(i) \overline{x}^*(i-1)$$

for each user will produce performance much closer to the ML-phase estimator given in [8]. In this way the set accuracy of the frequency sources can be less stringently specified and the system cost can be reduced while maintaining rapid acquisition.

Several characteristics of the EW estimator provide insight into the combined algorithm performance. A quantity of interest for the EW algorithm is the SNR gain, $G(n)$. For

the EW estimator, $G(n)$ is given by [6]

$$G(n) = \frac{(1-\beta^n)^2(1+\beta)}{(1-\beta^{2n})(1-\beta)}. \quad (5)$$

A disadvantage of the EW estimator is its inability to compensate for a frequency offset. So if the estimate of k was not included in the combined algorithm, a phase error bias would occur. This bias is given by

$$\theta_e(n) = \arg\left[\frac{1-(\beta k^{-1})^n}{1-\beta k^{-1}} k^{-1}\right] \quad (6)$$

and the corresponding gain is

$$G(n) = \frac{|1-(\beta k^{-1})^n|^2(1-\beta^2)}{|1-\beta k^{-1}|^2(1-\beta^{2n})}. \quad (7)$$

These quantities combined with results in Section IV provide methods to approximately calculate the BEP during acquisition.

Finally, the combined algorithm is a nonconstant modulus algorithm. The only advantage of this algorithm is the absence of hang-up [4], [5] when utilized with an unmodulated carrier or a training preamble. Otherwise, BPSK and QPSK demodulators are transparent to the reference signal magnitude.

IV. BEP Performance

A. BPSK and QPSK BEP with Noisy Complex Gaussian References

Optimum (in MAP sense) receivers of digitally modulated signals when the phase reference is random are a combination coherent receiver and square-law (noncoherent) receiver [15]. For BPSK and QPSK, a simplification is possible and the resulting receiver structures are

$$\hat{a} = \operatorname{sgn}[\operatorname{Re}(x(n)r^*(n))]$$
$$\hat{b} = \operatorname{sgn}[\operatorname{Im}(x(n)r^*(n))] \quad \text{(QPSK only)}$$

where $r(n)$ is the noisy phase reference.

The goal of this section is to quantify the equivalent BEP obtained during acquisition. Typically, burst-mode communication systems dedicate a preliminary portion of the burst to carrier acquisition.[5] During this preamble, the equivalent BEP is amenable to analysis. Since the matched filter output $x(n)$ and the reference signal $r(n)$ are complex Gaussian random processes (or accurately modeled as complex Gaussian), the problem can be analyzed with many well-known techniques.

In [17] a method particularly applicable to this problem was proposed. The BEP for the BPSK demodulator reduces to

$$P_B(E) = P(\operatorname{Re}[x(n)r^*(n)] \le 0).$$

Assuming both $x(n)$ and $r(n)$ are complex Gaussian signals and recalling the definition of the reference SNR gain $G(n)$ the BEP performance of the BPSK receiver with no phase reference bias can be calculated by [17]

$$P_B(E) = \frac{1}{2}\left[1 - Q\left(\sqrt{r_2}, \sqrt{r_1}\right) + Q\left(\sqrt{r_1}, \sqrt{r_2}\right)\right] \quad (8)$$

[5]The work in [11] is an exception but it has degraded performance with frequency offset.

where

$$Q(a,b) = \int_b^\infty x \exp\left[-\left(\frac{a^2+x^2}{2}\right)\right] I_0(ax)\,dx$$

is the Marcum Q-function and[6]

$$r_1 = \frac{1}{2}(\sqrt{GR_s} - \sqrt{R_s})^2$$
$$r_2 = \frac{1}{2}(\sqrt{GR_s} + \sqrt{R_s})^2$$

where $R_s = E_b/N_0$.

Calculation of the BEP of a QPSK receiver with a noisy Gaussian phase reference can again be accomplished using Stein's method [17]. Since the noise is rotationally invariant and the quadrature modulation symbols are independent, the BEP can be expressed as

$$P_Q(E) = \frac{1}{2}P[\operatorname{Re}[x(n)r^*(n)] \le 0] + \frac{1}{2}P[\operatorname{Im}[x(n)r^*(n)] \le 0].$$

Using the same procedure as used to derive (8), the QPSK BEP can be expressed as

$$P_Q(E) = \frac{1}{2}\left[1 - Q\left(\sqrt{r_4}, \sqrt{r_3}\right) + Q\left(\sqrt{r_3}, \sqrt{r_4}\right)\right] \quad (9)$$

where

$$r_3 = \frac{1}{2}\left[GR_s + R_s - R_s\sqrt{2G}\right]$$
$$r_4 = \frac{1}{2}\left[GR_s + R_s + R_s\sqrt{2G}\right]$$
$$R_s = E_s/N_0 = 2E_b/N_0.$$

The results in (8) and (9) can be studied to determine the interaction between the reference gain G and the BEP.

B. Acquisition BEP with Prior Frequency Estimation

This section will present the BEP learning curve. The BEP learning curve is simply a plot of the equivalent BEP as a function of symbol number after the start of acquisition. This curve is important in the design of FH or TDMA communication systems utilizing decision-directed carrier synchronizers. Examination of these curves provides one method of selecting the carrier acquisition preamble length. The BEP performance analyzed in this subsection corresponds to either the performance of the EW phase estimator with negligible frequency offset or the combined algorithm with an accurate prior estimate of k. In this case, the BEP learning curves will be a function of the R_s, β, and the symbol number. Since the reference SNR gain of the EW estimator is given in (5), the use of this result in (8) and (9) produces the BEP learning curves for BPSK and QPSK, respectively. These learning curves are plotted in Figs. 8–9. These figures demonstrate, in agreement with [19], that only a few symbols are needed to produce near-ideal BEP performance for BPSK and QPSK modulations with digital carrier synchronizers.

[6]When $G(n)$ is not an explicit function of n, we will use G.

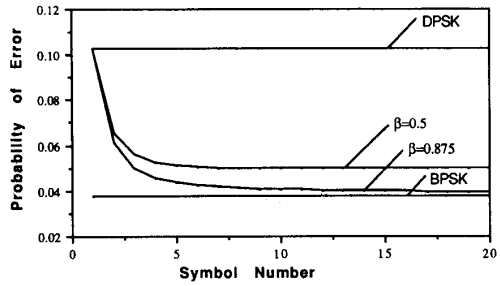

Fig. 8. BEP learning curve of the EW algorithm for BPSK modulation. $E_b/N_0 = 2$ dB.

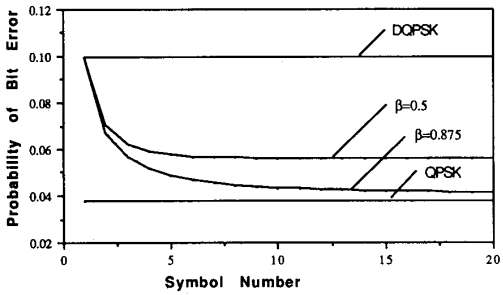

Fig. 9. BEP learning curve of the EW algorithm for QPSK modulation. $E_b/N_0 = 2$ dB.

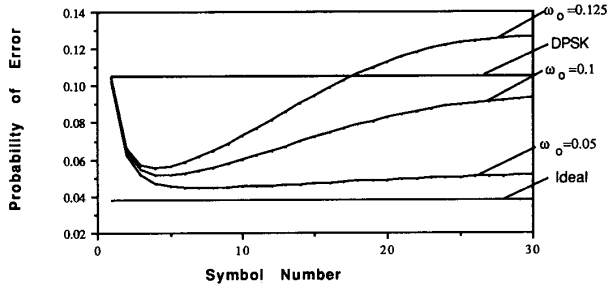

Fig. 10. BEP learning curve of the EW algorithm for BPSK modulation with frequency offset. $\beta = 0.875$, $E_b/N_0 = 2$ dB

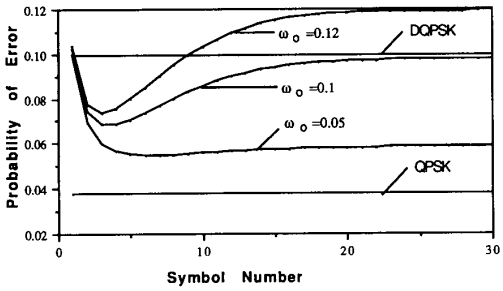

Fig. 11. BEP learning curve of the EW algorithm for QPSK modulation with frequency offset. $\beta = 0.875$, $E_b/N_0 = 2$ dB.

C. Acquisition BEP With No Frequency Estimation

As was shown in Section III-D the EW algorithm develops a phase bias in the presence of a frequency offset. This section will analyze the BEP performance of BPSK and QPSK when utilizing this algorithm. In performing this analysis the first point to realize is that the phase estimate is still a complex Gaussian process. To calculate the BEP we again use Stein's method [17] to get

$$P_B(E) = \frac{1}{2}\left[1 - Q\left(\sqrt{r_6}, \sqrt{r_5}\right) + Q\left(\sqrt{r_5}, \sqrt{r_6}\right)\right] \quad (10)$$

where[7]

$$r_5 = \frac{\rho^2(\omega_0)}{2}\left[GR_s + R_s - 2R_s\sqrt{G}\cos(\theta_e)\right]$$
$$r_6 = \frac{\rho^2(\omega_0)}{2}\left[GR_s + R_s + 2R_s\sqrt{G}\cos(\theta_e)\right].$$

The phase estimation bias θ_e is given by (6) while the reference SNR gain G is given by (7). Consequently, the BEP learning curves of BPSK utilizing the EW estimator when the input signal has a frequency offset are derived by substituting these factors into (10). Figs. 10–11 show these curves for various frequency offsets. As can be seen from the figure for each value of β there are frequency offsets at which the steady-state BEP performance of the EW estimator becomes worse than a DPSK demodulator. The cause of this degradation is the phase estimate bias developed by the EW algorithm. These frequency offsets at which the estimator becomes ineffective are lower for higher values of β. In a channel with no frequency uncertainty, increasing β improves BEP performance by averaging the received complex sinusoid over more symbols. When a frequency offset is present, the larger β is, the larger the phase estimation bias. This bias degrades the performance, while the increased averaging improves that performance. Essentially this implies that for each frequency offset there should exist an optimum value for β which would minimize the BEP. A very similar characteristic is exhibited when the correlation time of the phase noise process is shorter than the effective window length of the phase estimator. These characteristics are important to consider during the system design and analysis.

The BEP learning curves for QPSK can be derived in a similar manner using the methods developed in Section IV-B. The BEP of QPSK is given by (9) and for a phase error bias θ_e the reference signal will have the form

$$r(n) = \sqrt{GE_s}\exp[j(\theta + \theta_e)] + \nu_r(n)$$

while the matched filter output for $a_n = 1$ and $b_n = 1$ has the form

$$x(n) = \sqrt{E_s}\exp\left[j\left(\frac{\pi}{4} + \theta\right)\right] + \nu(n).$$

Using the results in [17] the conditional BEP reduces to

$$P_Q(E) = \frac{1}{2} - \frac{1}{4}Q\left(\sqrt{r_8}, \sqrt{r_7}\right) + \frac{1}{4}Q\left(\sqrt{r_7}, \sqrt{r_8}\right) - \frac{1}{4}Q\left(\sqrt{r_{10}}, \sqrt{r_9}\right) + \frac{1}{4}Q\left(\sqrt{r_9}, \sqrt{r_{10}}\right) \quad (11)$$

[7]Also, when $\theta_e(n)$ is not an explicit function of n we will use θ_e.

where

$$r_7 = \frac{\rho^2(\omega_0)}{2}\left[GR_s + R_s - 2R_s\sqrt{G}\cos\left(\frac{\pi}{4} + \theta_e\right)\right]$$

$$r_8 = \frac{\rho^2(\omega_0)}{2}\left[GR_s + R_s + 2R_s\sqrt{G}\cos\left(\frac{\pi}{4} + \theta_e\right)\right]$$

$$r_9 = \frac{\rho^2(\omega_0)}{2}\left[GR_s + R_s - 2R_s\sqrt{G}\cos\left(\frac{\pi}{4} - \theta_e\right)\right]$$

$$r_{10} = \frac{\rho^2(\omega_0)}{2}\left[GR_s + R_s + 2R_s\sqrt{G}\cos\left(\frac{\pi}{4} - \theta_e\right)\right].$$

Using (6) and (7) in (11) produces the desired BEP learning curves for QPSK. Fig. 11 shows these curves for various frequency offsets. As expected the sensitivity of QPSK to a phase reference bias is greater than BPSK. These results are important to consider when trying to gain the additional performance available with near coherent demodulation.

An interesting extension of (11) is the simple calculation of the BEP of a DQPSK demodulator in the presence of a frequency offset. This BEP can be determined by substituting

$$r_{7'} = R_s\rho^2(\omega_0)\left[1 - \cos\left(\frac{\pi}{4} + \omega_o\right)\right]$$

$$r_{8'} = R_s\rho^2(\omega_0)\left[1 + \cos\left(\frac{\pi}{4} + \omega_o\right)\right]$$

$$r_{9'} = R_s\rho^2(\omega_0)\left[1 - \cos\left(\frac{\pi}{4} - \omega_o\right)\right]$$

$$r_{10'} = R_s\rho^2(\omega_0)\left[1 + \cos\left(\frac{\pi}{4} - \omega_o\right)\right]$$

into (11). This appears to the authors to be an alternate method to that derived in [20] using results from [18].

D. Combined Algorithm BEP Acquisition Characteristics

The BEP performance evaluated in this section corresponds to a receiver which uses the combined algorithm presented in Section III-A to obtain a phase reference. Since the combined algorithm utilizes nonlinear processing, an analysis is not tractable. For this reason, Monte Carlo simulation was used to evaluate the BEP learning curves for the combined algorithm. Fig. 12 shows the simulated BEP learning curves for BPSK modulation of this algorithm. Fig. 12 demonstrates that $\beta = 0.75$ is near optimum exponential weighting for steady state BEP performance at $R_b = 2$ dB ($R_b = E_b/N_0$). Fig. 13 are the identical curves for QPSK modulation. It should be noted that these curves correspond to the performance during an unmodulated or training preamble. The effects of decision errors on the performance will be considered in Section IV-E.

E. Combined Algorithm with Decision Errors

Decision errors will degrade the performance of a decision-directed carrier synchronization subsystem. For the EW phase

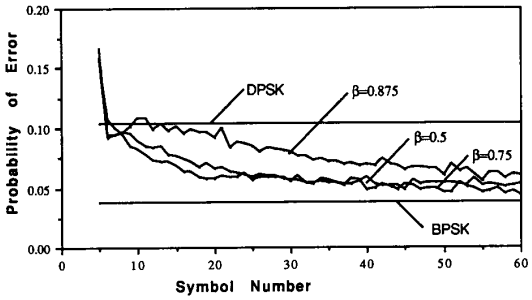

Fig. 12. BEP learning curve of the combined algorithm for BPSK modulation. $E_b/N_0 = 2$ dB, $kk = 4$, 10 000 Monte Carlo trials, $\omega_0 = 1.0$ radian/sample.

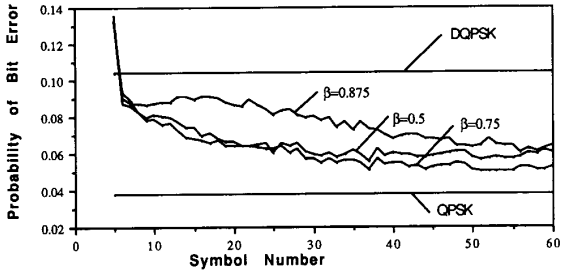

Fig. 13. BEP learning curve of the combined algorithm for QPSK modulation. $E_b/N_0 = 2$ dB, $kk = 4$, 10 000 Monte Carlo trials, $\omega_0 = 1.0$ radian/sample.

estimator, a nonlinear statistical analysis is possible and is given in [22]. The combined algorithm is not amenable to analysis, hence the effect of decision errors will again be evaluated by Monte Carlo simulation.

BPSK and QPSK constellations exhibit quadrant symmetry so multiple stable "lock" points exist. It is possible (at low SNR likely) to slip from one "lock" point to another. This slipping phenomena is partially compensated for by differential encoding of the transmitted data. Figs. 14–15 present the BEP waterfall curves with differential decoding derived from the Monte Carlo simulation. A simple Monte Carlo trial consisted of a 60-symbol burst, where four symbols were devoted solely to frequency estimation ($kk = 4$) and 5 symbols to phase estimate smoothing. The remaining 51 symbols were randomly modulated symbols. The BEP plotted in the figures is the average over this 51 symbol interval and each Monte Carlo trial.

Figs. 14–15 demonstrate the combined algorithm produces the desired results. For BPSK with $R_b = 2$ dB, the performance is within 1 dB of ideal, while at $R_b = 6$ dB, the performance is within 0.3 dB of ideal for a frequency offset of 0.5 radians per symbol. The QPSK performance is about 1.0 dB degraded over the regions of interest. Causes of this reduced performance include the increased sensitivity to noisy phase references and a higher probability of slipping inherent in QPSK modulation. The combined algorithm produces a rapidly acquiring ($\approx$ 9 symbols), high performance phase estimator analogous to a Type II PLL.

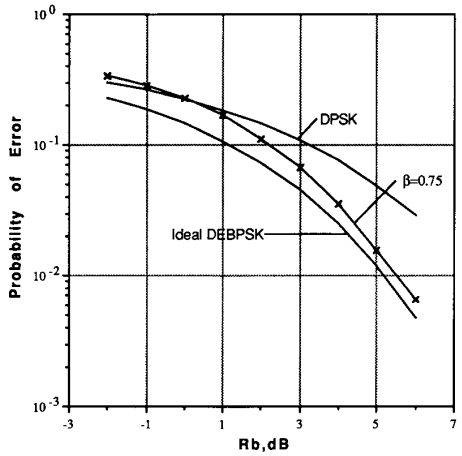

Fig. 14. BEP of differentially encoded BPSK modulation with a decision-directed combined algorithm phase estimator. Nine symbol training preamble ($kk = 4$), $\beta = 0.75$ 10 000 Monte Carlo trials, $\omega_0 = 1.0$ radian/sample.

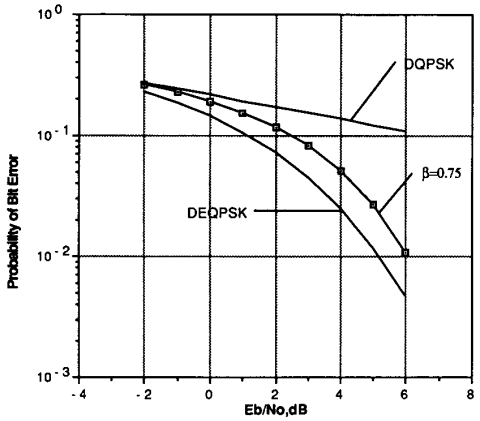

Fig. 15. BEP of differentially encoded QPSK modulation with a decision-directed combined algorithm phase estimator. Nine symbol training preamble ($kk = 4$), $\beta = 0.75$ 10 000 Monte Carlo trials, $\omega_0 = 1.0$ radian/sample.

V. Conclusion

Two major conclusions can be reached from this work. First, in channels where the correlation time of the channel phase process is long relative to the symbol duration, digital signal processing architectures exist which can rapidly acquire and track the phase and frequency. If the carrier frequency is accurately known then the EW algorithm can acquire a reference in less than 5 symbols. For reasonable E_b/N_0 and an unknown frequency, the combined algorithm provides reliable carrier synchronization in approximately 9 symbols. Improved performance can be obtained with longer preambles. Finally, Stein's method [17] provides a powerful analysis tool for evaluating the approximate degradation to BEP for data-aided implementations of these carrier phase estimation structures. This method has recently been generalized by Lindsey and Biyari [23], [24] and applied to the problem of diversity reception over nonzero mean, complex non-Gaussian, noisy channels; the complex Gaussian being a special case.

References

[1] W. C. Lindsey and M. K. Simon, *Telecommunications Systems Engineering.* Englewood Cliffs, NJ: Prentice-Hall, 1973.
[2] S. T. Alexander, *Adaptive Signal Processing.* New York: Springer-Verlag, 1986.
[3] S. S. Haykin, *Adaptive Filter Theory.* Englewood Cliffs, NJ: Prentice-Hall, 1986.
[4] F. M. Gardner, "Hangup in phase-lock loops," *IEEE Trans. Commun.,* vol. COM-25, pp. 1210–1214, Oct. 1977.
[5] H. Meyr and L. Popken, "Phase acquisition statistics for phase locked loops," *IEEE Trans. Commun.,* vol. COM-28, pp. 1365–1372, Aug. 1980.
[6] M. P. Fitz, "Open loop techniques for carrier synchronization," Ph.D dissertation, Univ. of Southern California, Los Angeles, CA, June 1989.
[7] P. Y. Kam, "Maximum likelihood carrier phase recovery for linear suppressed-carrier digital data modulations," *IEEE Trans. Commun.,* vol. COM-34, pp. 522–527, June 1986.
[8] A. J. Viterbi, *Principles of Coherent Communication.* New York: McGraw-Hill, 1966.
[9] J. G. Proakis, P. R. Drouilhet, Jr., and R. Price, "Performance of coherent detection systems using decision-directed channel measurement," *IEEE Trans. Commun.,* vol. COM-12, pp. 54–63, March 1964.
[10] F. M. Gardner, "Carrier and clock synchronization for TDMA digital communications," ESA Rep., June 1974.

[11] A. J. Viterbi and A. M. Viterbi, "Nonlinear estimation of PSK modulated carrier phase with application to burst digital transmission," *IEEE Trans. Inform. Theory,* vol. IT-32, pp. 543–551, July 1983.
[12] R. Haeb and H. Meyr, "A systematic approach to carrier recovery and detection of digitally phase modulated signals on fading channels," *IEEE Trans. Commun.,* vol. 35, pp. 748–754, July 1989.
[13] A. Aghamohammadi, H. Meyr, and G. Ascheid, "Adaptive synchronization and channel parameter estimation using an extended Kalman filter," *IEEE Trans. Commun.,* vol. 37, pp. 1212–1219, Nov. 1989.
[14] W. B. Davenport and W. L. Root, *An Introduction to the Theory of Random Signals and Noise.* New York: McGraw-Hill 1954.
[15] H. L. VanTrees, *Detection, Estimation, and Modulation Theory, Vol. 1.* New York: Wiley, 1968.
[16] J. C. Henry III, "DPSK versus FSK with frequency uncertainty," *IEEE Trans. Commun. Technol.,* vol. COM-18, pp. 814–816, Dec. 1970.
[17] S. Stein, "Unified analysis of certain coherent and noncoherent binary communications systems," *IEEE Trans. Inform. Theory,* vol. IT-10, pp. 43–51, Jan. 1964.
[18] R. F. Pawula, S. O. Rice, and J. H. Roberts. "Distribution of the phase angle between two vectors perturbed by Gaussian noise," *IEEE Trans. Commun.,* vol. COM-30, pp. 1828–1841, Aug. 1982.
[19] N. Liskov and R. Curtis, "Performance of coherent phase and amplitude digital modulations with carrier recovery noise," *IEEE Trans. Commun.,* vol. COM-35, pp. 972–976, Sept. 1987.
[20] M. K. Simon and D. Divsalar, "Doppler-corrected differential detection of MPSK," *IEEE Trans. Commun.,* vol. 37, pp. 99–109, Feb. 1989.
[21] H. V. Poor, *An Introduction to Signal Detection and Estimation.* New York: Springer-Verlag, 1988.
[22] M. P. Fitz and W. C. Lindsey, "A Markov analysis of decision-directed digital carrier synchronizers," *IEEE Trans. Commun.,* submitted for publication.
[23] W. C. Lindsey and K. H. Biyari, "Binary communication through non-Gaussian, noisy channels," *IEEE Trans. Inform. Theory,* submitted for publication.
[24] K. H. Biyari and W. C. Lindsey, "Diversity reception through complex non-Gaussian, noisy channels," *IEEE Trans. Commun.,* submitted for publication.
[25] G. W. Lank, I. S. Reed, and G. E. Pollon, "A semicoherent detection and Doppler estimation statistic," *IEEE Trans. Aerosp. Electron. Syst.,* vol. AES-9, pp. 151–165, Mar. 1973.

Michael P. Fitz (S'82–M'89) was born on December 1, 1960, in Akron, OH. He received the B.E.E. degree (summa cum laude) from the University of Dayton in 1983, and the M.S.E.E. and Ph.D. degrees from the University of Southern California in electrical engineering in 1984 and 1989, respectively.

While at USC he was a communication system engineer at both Hughes Aircraft Co., Fullerton, CA, and TRW Inc., Redondo Beach, CA. His responsibilities included the design, analysis, and testing of both satellite and portable communication systems. In 1989 he ventured into academia and currently remains there as an Assistant Professor of Electrical Engineering at Purdue University. His current research interests include communication system synchronization, fading channel communications, and equalization techniques.

William C. Lindsey (S'61–M'63–SM–'73–F'74) is Professor of Electrical Engineering at the University of Southern California, and serves as Chairman of the Board of LinCom Corporation which he founded in 1974. He has been a frequent consultant to government and industry. He has published numerous papers on varied topics in communication theory and holds several patents. He has written two books: *Synchronization Systems in Communication and Control* (Englewood Cliffs, NJ: Prentice-Hall, 1972) and *Telecommunication Systems Engineering,* coauthored with M. K. Simon (Englewood Cliffs, NJ: Prentice-Hall, 1973; revised edition, Dover Publications, 1991). He is also coauthor of the IEEE Press Book *Phase-Locked Loops and Their Applications.*

Dr. Lindsey serves on Commission C, Signals and Systems of the International Scientific Radio Union (URSI) and was Vice President for Technical Affairs of the IEEE Communications Society. He also served as the second chairman of the Communication Society Committee and is a former Editor of ComSoc.